

Performance Characteristics of a Linear Ionic Liquid Electro spray Thruster

IEPC-2005-192

Presented at the 29th International Electric Propulsion Conference, Princeton University,
October 31 – November 4, 2005

Paulo Lozano^{*}, Benajmin Glass[†] and Manuel Martinez-Sanchez[‡]
Massachusetts Institute of Technology, Cambridge, MA, 02139, USA

Abstract: A laboratory-type micropropulsion thruster has been built based on the electrostatic field evaporation of ions from the ionic liquid EMI-BF₄. Liquid transport from the reservoir is achieved solely by capillary forces over the surface of the emitter. The device is comprised of 31 individual solid emitters, electrochemically treated to improve wetting and to generate sharp edges from which ion emission can be achieved at relatively low voltages. The emitters are produced from 70 μm thick by 0.9 mm wide tungsten filaments. This geometry allows an increase of over one order of magnitude in emission current compared to cylindrical emitters. The filaments are positioned side-by-side generating a line from which emission occurs. Currents as high as hundreds of μA are typical with this arrangement at voltages between 1.5 and 3 kV. The plume has been characterized using time-of-flight spectrometry and retarding potential analyzer instruments, showing that pure ion emission is achieved with very narrow energy distributions (~10 eV) at potentials just barely below (by 0.5 to 1%) the applied voltage.

Nomenclature

c	= ion exhaust velocity
F	= engine thrust
I	= ion beam current
L	= drift distance in the time-of-flight spectrometer
m	= particle mass
\dot{m}	= mass flow rate
q	= particle electric charge
t	= time of flight over drift distance
V_0	= applied voltage
$\Delta\phi$	= potential spread due to beam angular divergence
ϕ_0	= nominal on-axis accelerating potential
θ	= beam spreading half-angle

I. Introduction

ELECTROSPRAY thrusters are devices that make use of liquid phase ionization to produce and accelerate streams of molecular ions and/or highly charged droplets to high velocities. The production of these charged entities is based on the Taylor cone effect in which a conductive liquid is stressed under the presence of an externally applied electric field thus producing a surface instability that grows until a stable cone-like structure is

^{*} Research Scientist, Aeronautics and Astronautics, plozano@mit.edu.

[†] Junior year student, Aeronautics and Astronautics, bwg@mit.edu.

[‡] Professor, Aeronautics and Astronautics, mmart@mit.edu.

formed.¹ Near the tip of this structure the electric fields are strong enough that the shape of the liquid departs from a perfect cone turning into a thin jet that breaks up into a spray of nano-sized droplets. Using the right combination of operating conditions and liquid properties, it is also possible to suppress the emission of droplets completely and produce a beam of singly-charged ions.² The ion emission mechanism (field evaporation) is very similar to that encountered in field emission electric propulsion thrusters (FEEP) and liquid metal ion sources (LMIS).

Electrospray thrusters are attractive for many reasons, in particular their intrinsic small size makes them ideal for micro/nano satellites. The thrust produced by each Taylor cone emitter is very small, and therefore a number of them need to be stacked in parallel. Missions that require very fine impulse maneuvers would also benefit from this technology, such as the DRS ST-7 or LISA missions in which micro-N level thrust is required to compensate for external orbit perturbations. In addition, electrospray thrusters appear to be highly efficient, especially in the purely ionic mode. Energy analyses on single emitters show that the ionic species are accelerated practically to the full applied potential with very narrow distributions around it.³ Being a cold emission type of ionization, no thermal motion of the particles is produced, creating a plume beam contained in well-defined cones with half-angles below 20° to 30° degrees from the centerline.⁴

Among the many architectures proposed for these thrusters, we have selected one in which the propellant is passively transported from the reservoir to the emitter tips through external capillarity forces alone. The liquid is therefore exposed to vacuum conditions, but operation is possible if the propellant is an ionic liquid, a kind of organic-inorganic salt, which remains in the liquid, phase at room temperatures and lower. These ionic liquids have negligible vapor pressure, are resistant to significant doses of radiation,⁵ are stable at high temperatures and have a relatively high electrical conductivity, making them suitable for their use in an electrospray thruster. The ionic liquid EMI-BF₄ has been selected for this study since it has been widely characterized as a thruster propellant and is therefore suitable to make relevant comparisons between the emitter type used here and those described elsewhere.^{2,4}

The thruster has been characterized in terms of its current versus voltage response, its ionic composition and energy distribution of emitted particles. This allows us to estimate thrust. Direct characterization still is required and some other design and operational issues need to be resolved, like the interception of current by the extractor, which as will be described shortly, represents about 20% of the total current. Nevertheless the thruster architecture is appealing because of its simplicity and ability to achieve larger current densities than other types of field evaporation thrusters at moderate voltages.

II. Thruster Design and Fabrication

The fundamental approach taken in the thruster design is to use flat, foil-like tungsten filaments treated to increase wettability by the ionic liquid and electrochemically etched to produce anchoring sites over which the Taylor cones can be produced. The reason for selecting this geometry instead of that based on cylindrical emitters is that for similar cross-section perimeters, the current obtained using flat filaments is about an order of magnitude higher. These emitters appear to have much better liquid transport properties when their surfaces have been properly treated, allowing them to operate over wide ranges of voltages with no liquid starvation.

The emitter fabrication procedure is analogous to that used in cylindrical needles.⁴ The ionic liquid would not normally wet untreated, smooth tungsten. However, from the way the filaments are produced, there is some degree of roughness preferentially aligned along the filament length. In addition, the oxide layer covering the raw material is removed using a 10 sec, 5 VAC electrochemical bath under a 1N solution of NaOH using a stainless steel counter-electrode. To produce the emitting tip, the tungsten filament is partially submerged (about 3 mm) under the solution surface and 50 VDC are applied between it and the counter-electrode. In a few seconds the tungsten dissolves electrochemically, leaving a sharp edge that is then smoothed out using 10 VAC. The final step involves a chemical attack of the surface

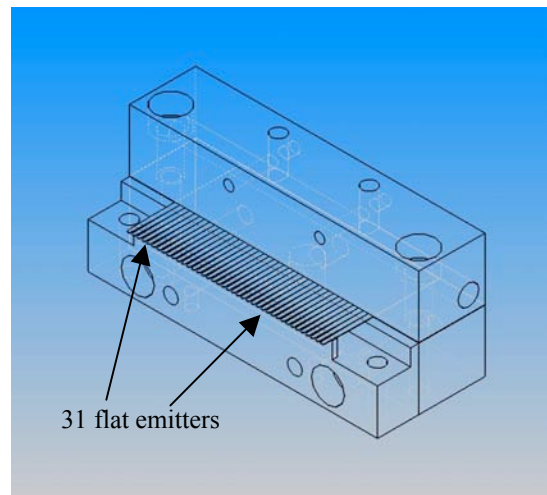


Figure 1. Sketch of the linear thruster displaying the emitter locations and supporting structure.

using a hot saturated solution of potassium ferricyanide under 2N NaOH for 45 sec. This creates a very thin porous layer over the tungsten surface, improving considerably the wetting properties. The emitters are ultrasonically cleaned immediately after the chemical attack using alternating deionized water and acetone baths.

The thruster body consists of four metallic parts (blocks), which are fastened together using machine screws. The 31 emitters are installed over the surface of the lower rear block (10 x 9.5 x 44 mm) using double-sided conductive tape. The upper rear block (same dimensions) is fastened on top of the emitters to clamp them in place. Finally the lower and upper front blocks (6.4 x 9.5 x 44 mm) are fastened together. The purpose of these last pieces is to assure a good alignment of the thin filaments in the transversal direction and also they serve as propellant reservoir once the emitters are wetted. The extractor has a 38 mm wide and 0.76 mm thick slit and is mounted over the front blocks using 2.5 mm alumina spacers and Teflon screws. The distance between emitter tips and the slit entrance is 0.8 mm. A drawing of the semi-complete thruster is shown in Fig. 1, while Fig. 2 shows a couple of photographs of the assembled thruster with and without the extractor electrode.

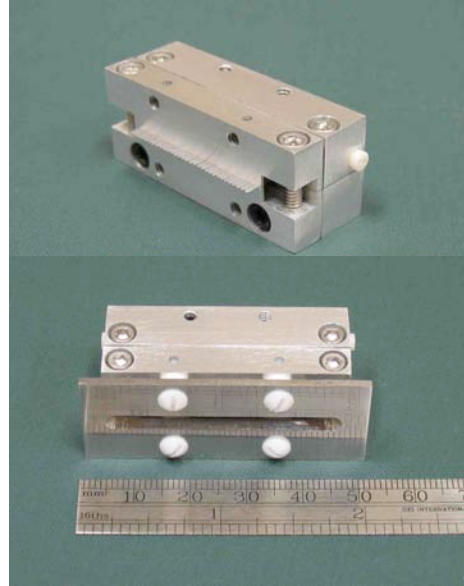


Figure 2. Two views of the assembled thruster, with and without the extractor electrode.

The emitters are wetted with EMI-BF₄ by depositing a small drop on both sides of each one of them. The liquid spreads out rapidly along the surface and finally rests on the interface between the filaments and the front blocks, effectively turning into the liquid reservoir of the thruster. To produce charged emission, a voltage V_0 is applied to the body of the thruster (which is electrically connected to the tungsten filaments and therefore to the ionic liquid) with respect to the grounded extractor.

III. Experimental Techniques

The device is tested in a turbopumped 140 ls⁻¹ vacuum chamber at pressures of about 1x10⁻⁶ Torr. Three instruments were used in the present study to characterize the performance of the thruster: (1) a large collector plate localized 4 cm away from the extractor to detect the full beam current, (2) a time-of-flight spectrometer to determine the beam composition and (3) a multi-grid retarding potential analyzer (RPA) to measure the energy distributions of the emitted species. In all cases a highly transparent metallic grid situated 3 mm in front of the detectors was used to suppress electron secondary emission, which can be considerable given the high energies of the emitted particles. The TOF apparatus measures the drift time of particles towards the detector over a given distance $L = 747$ mm as measured from an interleaved wire electrostatic deflector and the detector surface, consisting of a Faraday cup 38 mm in diameter. The small size of the detector compared to the drift length means that only those particles traveling axially would hit the collecting surface. It is known that beams produced by electrospray sources are well contained in conical distributions with half angles θ between 20° and 30°, therefore an ion focusing element (einzel lens) was added to the system to increase the signal level. Deflection plates are also included to steer the beam and guide it to obtain the highest current value for the TOF measurements.

The RPA is used to measure the energy distributions, or the accelerating potential ϕ_0 of the beam species. A complete description of the device can be found elsewhere.⁶ This information combined with the TOF results (drift time, t) allows us to determine the beam composition in terms of the mass per unit charge m/q ,

$$\frac{m}{q} = \frac{2\phi_0 t^2}{L^2}. \quad (1)$$

The RPA also includes ion optics elements to collimate the beam and therefore eliminate the electric potential spreads that normally appear in planar RPA instruments when studying divergent beams,

$$\Delta\phi/\phi_0 = \sin^2 \theta. \quad (2)$$

The thruster was tested with positive and negative voltages using a bipolar high-voltage amplifier. Previous studies have determined that prolonged DC operation induces electrochemical reactions and possible degradation of the liquid and surfaces. This problem is solved by periodically alternating the power supply polarity at low frequencies (about 1 Hz).⁷ Furthermore, DC negative operation with EMI-BF₄ is possible since the reaction products leave in gaseous form apparently without interacting with the liquid or the emitter surface.

IV. Characterization Results

Figure 3 shows the total thruster output current vs. voltage (negative polarity). The starting voltage of about 1.4 kV is comparable to that of cylindrical needle emitters. It is seen also that currents as large as 180 μA can be obtained for voltages approaching 3 kV. To put this result in perspective, we have taken similar data from a 0.5 mm in diameter single needle emitter⁴ and multiplied them 31 times to construct an idealized 31-needle thruster. This curve is also shown in the figure. It can be observed that the amount of current obtained with the flat filament configuration is more than an order of magnitude higher. Furthermore, emission beyond 2 kV was very unstable and eventually not possible using cylindrical needles, while tests at even higher voltages were performed with the linear thruster in which no current saturation was observed, suggesting an exponential Schottky-type emission mechanism with no apparent liquid flow starvation. Currents as high as 300 μA were obtained in this way.

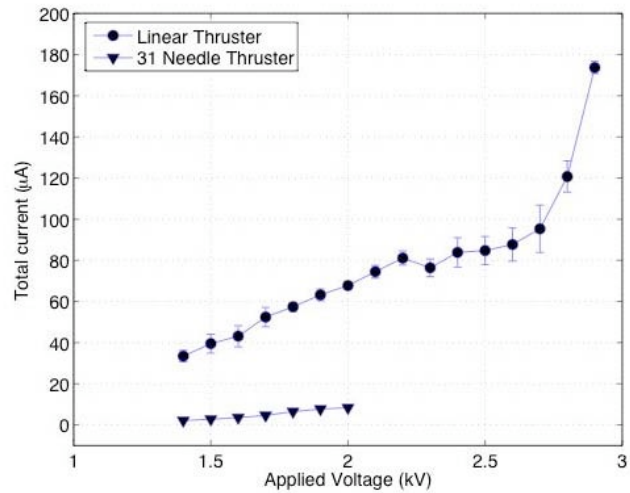


Figure 3. Current against voltage characteristics for the linear thruster and extrapolation to 31 single cylindrical emitters

The curve shown in Fig. 3 represent the total current going through the power supply, which was directly measured with an ammeter in series with the HV power supply. The current however, was also measured using the collector plate described in the previous section. Ideally both readings should be identical, or at most the one from the collector plate should be slightly lower due to particle interception by the electron-retarding grid. In practice however, the collected current represented about 80% of the total current. It appeared that 20% of the current was most likely lost to the extractor. To verify this, a second ammeter was connected in series with the extractor to monitor the current collected by it. It was found that about 20% of the current was passing through the extractor for the full range of voltages shown in the figure. Using this number together with the spacing

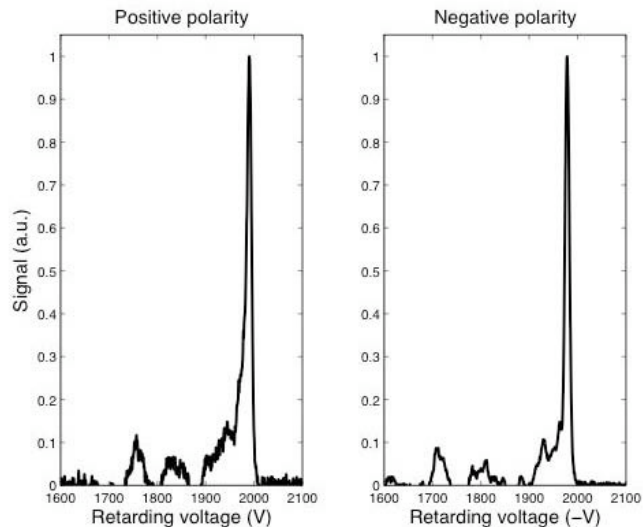


Figure 4. Positive and negative potential distributions with $V_0 = 2\text{kV}$ as measured with the RPA

between the emitter tips and the extractor and the slit width, it is possible to estimate an angular divergence between 25° and 30° from the centerline for the charged particle beam assuming uniform angular emission.

The energy distributions for positive and negative polarities are shown in Fig. 4 for an applied voltage $V_0 = 2$ kV. It can be seen that there is a prominent, sharp peak located very near the applied voltage for both cases. The widths (FWHM – full width at half maximum) of the peaks are 12 V for the positive spectrum and 11 V for the negative case. In addition, the accelerating potentials for positive and negative particles amount to 1990 V (or about 0.5% below V_0) and 1980 V (or 1% below V_0), respectively. These figures are very similar to those observed in FEEPs and in general for LMIS suggesting very high emission efficiency. There are also some smaller signatures observed at lower energies. These most likely come from the break up of metastable solvated ions as they gain velocity while still traveling in the acceleration region between the emitter tips and the extractor.⁶

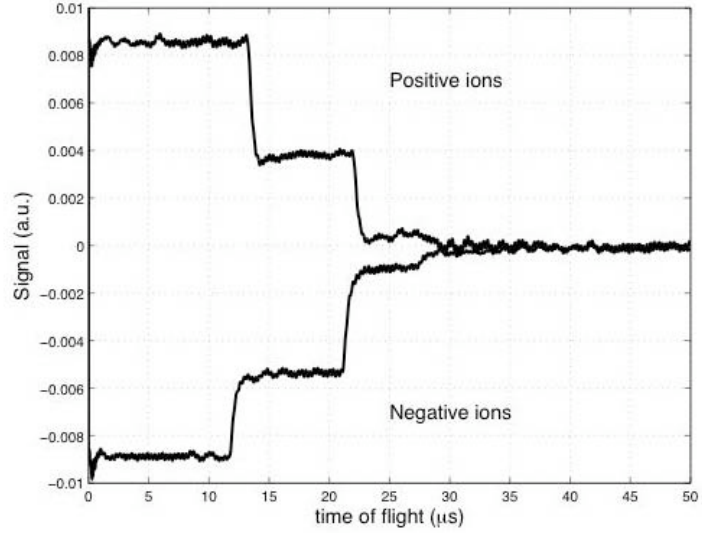


Figure 5. Bipolar TOF spectra with $V_0 = 1856$ V

The identity of the emitted species can now be determined using the TOF spectrometer. Figure 5 for instance, shows TOF curves for an applied voltage $V_0 = 1856$ V. Each step in the measured signal represents a different charged particle family. As mentioned in the last paragraph, the actual accelerating potentials are slightly lower than V_0 . Assuming that $\phi_0^+ = 0.995V_0$ and $\phi_0^- = 0.99V_0$, then we can use Eq. (1) to obtain the mass per unit charge of the different species. Assuming further that only singly charged particles are emitted, the actual masses can be computed and therefore the ions can be identified. The results of such exercise are summarized in Table 1. These ions and their relative abundances are very similar to those obtained with cylindrical needle emitters.^{2,4}

Table 1. Masses of ions as measured using TOF spectrometry with $L = 747$ mm and $V_0 = 1856$ V

Polarity	Time-of-flight, from Fig. 6 (μ s)	Mass, from Eq. (1) (amu)	Corresponding ion
Positive $\phi_0^+ = 1846.72$ V	13.2	111.2	EMI+
	22.0	308.8	(EMI-BF ₄)EMI+
	28.2	507.3	(EMI-BF ₄) ₂ EMI+
Negative $\phi_0^- = 1837.44$ V	11.8	88.38	BF ₄ -
	21.2	285.3	(EMI-BF ₄)BF ₄ -
	27.5	480.0	(EMI-BF ₄) ₂ BF ₄ -

This information can be combined to obtain an estimate of the thrust F produced by the linear engine (assuming once more uniform current emission below a half angle θ_0) after adding the individual contributions of each beam species,

$$F = \sum_i (\dot{m}_i c_i)_x = \sum_i I_i \sqrt{\frac{2m_i \phi_{0i}}{q}} \frac{\sin \theta_0}{\theta_0}, \quad (3)$$

where the x is introduced to emphasize that only the axial component of force produces thrust. If each particle family carries a constant fraction of the total current for every voltage and these fractions are those depicted in Fig. 5, then the I-V curve shown in Fig. 3 can be transformed directly to thrust. Assuming an adequate extractor design in which no ion interception occurs and assuming also a beam spreading half angle $\theta_0 = 25^\circ$ from the centerline, the

engine thrust varies from little more than 2 μN at 1.4 kV to 19 μN at 2.9 kV, or about 0.1 μN for each μA of output current.

V. Conclusion and Future Work

A simple electric micropropulsion thruster has been designed and tested based on the electrostatic extraction of solvated ions directly from externally wetted flat tungsten filaments using the non-volatile ionic liquid EMI-BF₄. The current emission density obtained with this configuration is over an order of magnitude higher than previous tests using cylindrical tungsten wire. The results presented in this work were obtained at room temperature. It is known, however that slight increases in temperature have a considerable effect on the amount of emitted current. For instance, for single needle emitters, the current increases 2 times when the temperature is increased from 20°C to 40°C.⁴ Our design incorporates a heating element that could eventually boost the current (hence the thrust) to even higher levels after providing moderate increases in temperature. Future work still needs to be done to reduce and eventually eliminate the current interception by the extractor. The main motivation of exploring this flat configuration is to extend its use from the linear metal-based concept presented here to bi-dimensional microfabricated array designs that could potentially offer much higher current densities that would allow these engines to produce more sizable thrusts.

Acknowledgments

Funding for this work was provided by AFOSR grant # FA9550-04-C-0118 monitored by M. Birkan. The authors would like to thank Steven Barrett from Cambridge University (UK) for his assistance in the initial stages of production of a single-blade (flat) tungsten-based thruster.

References

- ¹ Taylor G I 1964 Proc. R. Soc. Lond. A280 (1382) 383-97.
- ² Romero-Sanz I, Bocanegra R, Fernandez de la Mora J and Gamero-Castaño M 2003 J. Appl. Phys. 94 3599-605
- ³ Lozano P and Martinez-Sanchez M 2002 Proc. 41st Joint Propulsion Conf. (Tucson, Arizona) AIAA paper #2005-4388.
- ⁴ Lozano P and Martinez-Sanchez M 2005 J. Colloid Interface Sci. 282 415-21
- ⁵ Ziemer J K, Marrese-Reading C M, Anderson M, Plett G, Polk J, Gamero-Castano M and Hrubu V 2003 Proc. 39th Joint Propulsion Conf. (Huntsville, Alabama) AIAA paper #2003-4853.
- ⁶ P. Lozano, *Energy distributions and in-flight fragmentation of positive and negative ions emitted from an EMI-Im ionic liquid ion source*, Journal of Physics D: Applied Physics, submitted for publication (Sept. 2005).
- ⁷ Lozano P and Martinez-Sanchez M 2005 J. Colloid Interface Sci. 280 149-54